

Kinetic Model for Tensile Deformation of Polymers. 5. Effect of Temperature on Orientation Efficiency

Yves Termonia*[†] and Paul Smith[‡]

Central Research and Development, E. I. du Pont de Nemours and Company, Inc., Wilmington, Delaware 19880-0356, and Materials Department and Department of Chemical and Nuclear Engineering, University of California at Santa Barbara, Santa Barbara, California 93106

Received January 13, 1993; Revised Manuscript Received April 5, 1993

ABSTRACT: A previous molecular model for tensile deformation of polymers is extended to include the effect of temperature on the development of orientation during drawing of flexible polymers that are characterized by weak intersegmental interactions, such as polyethylene. The results obtained confirm the experimentally observed existence of a maximum drawing temperature above which the efficiency of the orientation process decreases, presumably due to disentangling and recoiling of the polymer chains. This maximum temperature is predicted to increase linearly with (the logarithm of) the weight-average molecular weight. Polydispersity was found to significantly decrease the efficiency of drawing at high temperatures.

Introduction

It is well known that certain flexible polymers can be drawn into highly oriented structures that have tensile moduli approaching the theoretical values for the single chains. This is particularly true for polymeric materials that are characterized by weak intersegmental interactions, such as polyethylene, isotactic polypropylene, etc. The various drawing techniques and the observed dependence of the modulus on draw ratio for high-density polyethylene have been recently summarized by Wang et al.¹ The maximum draw ratio, and therewith the maximum modulus achieved, is well known to be strongly influenced by a variety of parameters, such as the drawing temperature and rate, molecular weight distribution, and the method of material preparation. By contrast, it is found that the tensile modulus often shows a universal increase with draw ratio, essentially irrespective of the drawing technique, sample preparation method, and molecular weight.

In a recent set of publications,^{2,3} a two-state model was proposed to account for the above experimental observation of a unique modulus-draw ratio relation of a broad variety of flexible chain polymers. In this approach, the macromolecular chain is considered to be comprised of only two elastic elements: stiff, or "helix", elements which are perfectly oriented along the draw axis and soft, or "coil", elements which are unoriented. Use of the Kuhn and Grun⁴ expression for the orientation distribution allows the derivation of a simple analytical equation for the relation between the draw ratio and the tensile modulus. A major assumption in the approach of refs 2 and 3, however, is that the deformation proceeds in an affine manner, which is reasonable only at temperatures well below the melting point of the polymer. It is well established experimentally (e.g., refs 5-7), however, that at elevated temperatures, where the maximum draw ratio may be increased, the efficiency of the drawing process may be significantly reduced, leading to a less rapid increase of the modulus with draw ratio. In the present work, we extend a previously introduced molecular model for tensile deformation of flexible chain polymers⁸⁻¹⁰ to include the effect of temperature on the drawing efficiency. As in our earlier studies, linear polyethylene (PE) was chosen as the model system, and emphasis is placed on

qualitative correlations with experimental results, and not on fitting of model parameters.

The Model

Deformation. The reader is referred to refs 8-10 for a detailed description of the deformation model, its assumptions, and parameters. Following our previous approach, the macromolecular solid is represented by an array of polymer chains entangled along their contour. As this network is drawn, the entanglements move along the tensile axis, and orientation and extension of the chain strands are induced. The model allows for the chains to slip through entanglements. The latter process is assumed to be thermally activated and is described using Eyring's chemical reaction rate theory. Since the chain slippage process leads to a continuous redistribution of stress among the various chain segments (see refs 8-10 for details), it is in our model fully responsible for a nonaffine type of deformation. Chain slippage also leads to a change in the number of statistical segments, n_e , between entanglements and, occasionally, to chain disentanglement.

In contrast to our previous work,⁸⁻¹⁰ here we allow for disentangled chain ends to reentangle with neighboring chains. This is performed according to one of two processes. In process i (see Figure 1), two interpenetrating chain ends with number of segments larger than n_e reentangle to form two unstrained strands with end-to-end vector lengths of $r = n_e^{1/2}l$. In process (ii) (Figure 1), a single chain end of n segments is allowed to entangle with a neighboring chain strand in its middle point when the latter lies within its radius of gyration. This leads to the formation of an unstrained strand of $n' > n$ segments and end-to-end vector length $r' = n'^{1/2}l$. In all our simulations, we found that the algorithms described above lead to a number of chain disentanglements approximately equal to the number of chain "reentanglements", so that the total number of entanglements remains constant. Unless otherwise specified, our external deformation rate for the network is set at 2.8 min⁻¹. In the present work, for simplicity we restrict ourselves to single-stage drawing, i.e., to deformation processes carried out at a constant temperature, and are not concerned with so-called two-stage drawing at different temperatures or drawing in temperature gradients (cf. refs 11 and 12).

Modulus Calculation. At the desired draw ratio, deformation is arrested and the polymer network is "cooled

* E. I. du Pont de Nemours and Co., Inc.

† University of California at Santa Barbara.

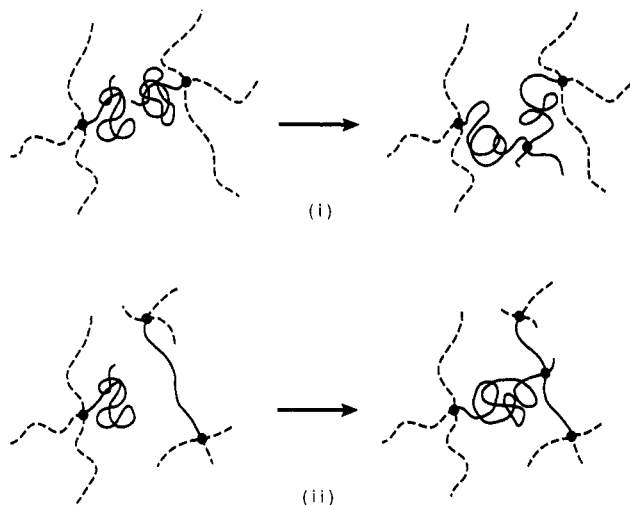


Figure 1. Two processes for chain reentangling. In process i, two interpenetrating chain ends with number of segments larger than n_e reentangle to form two unstrained strands with end-to-end vector lengths $r = n_e^{1/2}l$. In process ii, a single chain end of n segments is allowed to entangle with a neighboring chain strand in its middle point when the latter lies within its radius of gyration. This leads to the formation of an unstrained strand of $n' < n$ segments and end-to-end vector length $r' = n'^{1/2}l$.

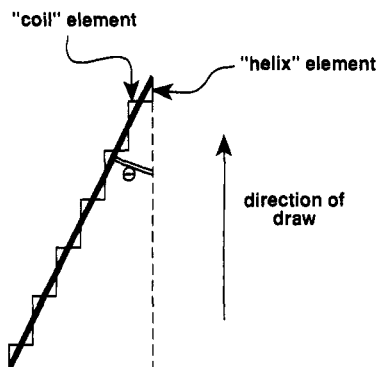


Figure 2. Two-state model representation of a chain strand between two entanglements. The strand forms an angle θ with the draw axis.

down" to room temperature. That "cooling down" is realized as follows. We start by replacing every chain strand between two entanglements by a string of only two elements: "helix" elements—denoted h —oriented along the draw axis and "coil" or unoriented elements, denoted u (see Figure 2). For a chain strand i having angle θ with the draw axis their respective fractions are given by

$$V_h = \cos \theta / (\sin \theta + \cos \theta) \quad (1a)$$

and

$$V_u = \sin \theta / (\sin \theta + \cos \theta) \quad (1b)$$

for the helix and coil elements, respectively. The elastic modulus of strand i along the draw axis is subsequently obtained from

$$E_i = [V_h/E_h + V_u/E_u]^{-1} \quad (2)$$

in which E_h and E_u are the moduli values for the two elements, as in refs 2 and 3. Thus, E_h ($=300$ GPa for PE) represents the axial tensile modulus of a defect-free crystal, and E_u ($=1.6$ GPa for PE) coincides with the shear modulus of the crystalline phase. A relation similar to eq 2 has been derived in refs 2 and 3 for the axial modulus of the *entire network* of polymer chains, assuming the deformation is affine. In the present approach, the assumption of homogeneous deformation is removed and

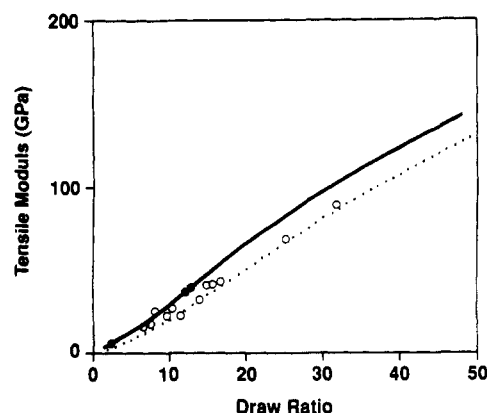


Figure 3. Development of tensile modulus with draw ratio for PE. The continuous curve represents our model predictions in the absence of entanglement slippage for a polymer with $M_w = 2.2 \times 10^6$ ($M_n = 1.6 \times 10^6$). The dotted line is calculated with the model of refs 2 and 3, assuming affine deformation. Open symbols (O) are experimental data taken from ref 13.

eq 2 is applied to *every single chain strand* of the network.

After assignment of axial and transverse moduli values for all the chain strands, the drawn polymer network is given an external extension of 1% along the draw axis. The network is then relaxed toward mechanical equilibrium and the axial tensile modulus is obtained from the average stresses at both ends.

A typical simulation of the model described above requires, depending on the system's parameters, a few hours of CPU time on a single 25-MHz processor of a 280-SGI server.

Results and Discussion

Figure 3 shows the calculated development of the tensile modulus with draw ratio in the *absence* of entanglement slippage. The data in this figure were obtained for an ultrahigh molecular weight (UHMW) PE of $M_w = 2.2 \times 10^6$ ($M_n = 1.6 \times 10^6$) and with a molecular weight between entanglements $M_e = 126 \times 10^3$ (which can be prepared experimentally by gelation-crystallization from a 1.6% v/v solution; see ref 8b). The maximum draw ratio for this material is ~ 50 .^{8b} The present calculations of the increase in modulus with draw ratio are in good agreement with those of the affine model of refs 2 and 3. This is not surprising since, in the absence of entanglement slippage, the deformation is in our model expected to be homogeneous, except for a minor nonaffine contribution stemming from the finite value of the molecular weight. Also represented in Figure 3 are experimental data taken from ref 12 for UHMW PE fibers with $M_w = 1.5 \times 10^6$, gel-spun from a 2% solution and drawn at 120 °C. The qualitative agreement with our model results is judged to be excellent, which leads to confidence in the validity of our two-state model (Figure 2 and eqs 1 and 2) and of the detailed algorithms for network relaxation.

Predictions of the effects of high drawing temperatures on the development of the modulus with draw ratio are presented in Figure 4. The results are, like those in Figure 3, for UHMW PE with $M_w = 2.2 \times 10^6$ ($M_n = 1.6 \times 10^6$). The data in this figure indicate that the increase in modulus with draw ratio is systematically reduced at deformation temperatures exceeding 105 °C. Interestingly, at a very high drawing temperature a *decrease* of the modulus is seen at high draw ratios, which, in fact, often has been found experimentally.

Further analysis of the calculations reveals that, at elevated temperatures, the polymer chains increasingly slip through entanglements, which leads to a substantial

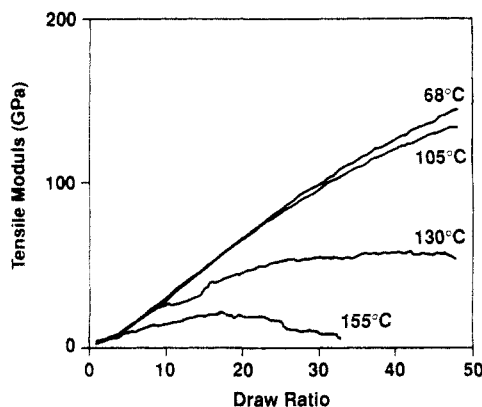


Figure 4. Calculated dependence of tensile modulus on draw ratio at high drawing temperatures. The figure is for PE with $M_w = 2.2 \times 10^6$ ($M_n = 1.6 \times 10^6$).

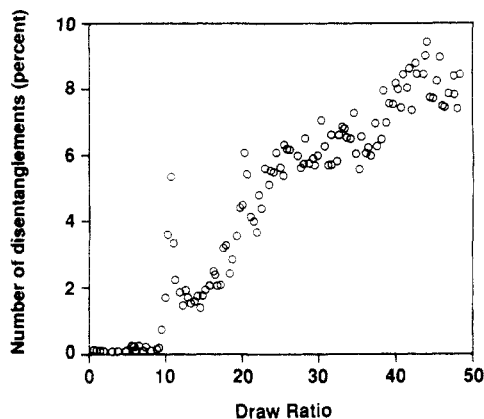


Figure 5. Calculated dependence of the number of disentanglements on draw ratio at $T = 130^\circ\text{C}$ for the polymer in Figure 4. The number is in percent of the total number of entanglements and for a fixed increment of draw.

amount of chain disentangling and recoiling. Figure 5 shows the dependence of the number of disentanglements on the draw ratio at $T = 130^\circ\text{C}$. This number is in percent of the total number of entanglements and for a fixed increment of draw of 0.25. Inspection of the figure shows that chain disentanglement mainly occurs at draw ratios $\lambda > 10$, at which we also start to observe (see Figure 4, 130°C) a significant slowing down in the increase of modulus with draw ratio. Note that the rate of chain disentanglement also steadily increases with draw at $\lambda > 10$. The fraction of disentangled nodes is rather small and never exceeds 10% of the total number of entanglements. However, any small amount of unoriented chain segments has a deleterious effect on the fiber modulus.

In agreement with experimental observations (cf. refs 5–7), the results of Figure 4 clearly point to the existence of a maximum temperature, T_{\max} , where tensile deformation is most efficient. That temperature, not unexpectedly, was found to be strongly dependent on molecular weight. Calculations of the development of the Young's modulus with draw ratio at various temperatures were carried out with the present model for molecular weights ranging from 10^5 to 10^7 . The results are given in the graph of Figure 6, where the heavy bars indicate the temperature range above which our model results predict a low efficiency of drawing. The data reveal an essentially linear increase of T_{\max} with (the logarithm of) the weight-average molecular weight, M_w . Also plotted in the graph of Figure 6 are experimentally determined maximum temperatures for efficient tensile deformation. The latter data were derived from various literature sources. The results presented in Figure 6 indicate that there is a qualitative

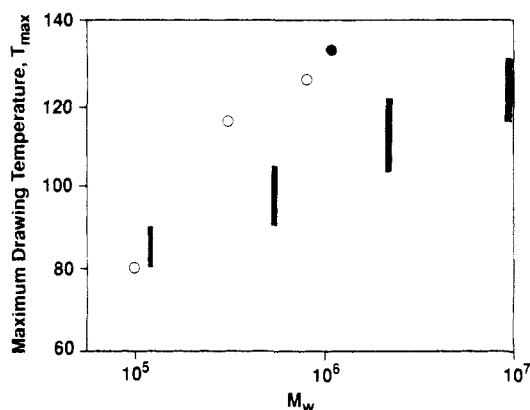


Figure 6. Dependence of the maximum drawing temperature (T_{\max}) on weight-average molecular weight (M_w). The heavy bars denote the predicted range. Experimental data are taken from refs 5 (○) and 7 (●).

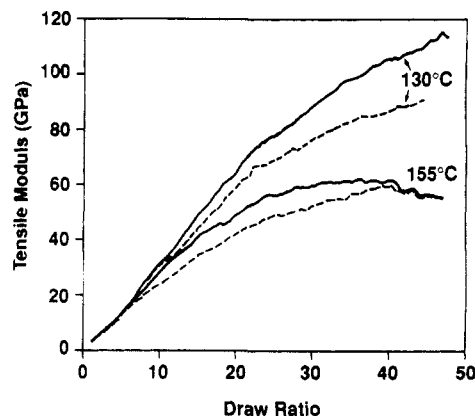


Figure 7. Effect of polydispersity on the calculated dependence of modulus on draw ratio at two different drawing temperatures: $T = 130$ and $T = 155^\circ\text{C}$. The continuous lines are for a monodisperse PE with $M_n = M_w = 9.2 \times 10^6$; the dashed lines are for a polydisperse PE with $M_n = 3.5 \times 10^6$ and $M_w = 9.4 \times 10^6$.

agreement between the present calculations and the experimental observations, the differences being the absolute values of T_{\max} and the slope of the M_w - T_{\max} curve. It should be stressed, however, that the sole purpose of the present work is to provide such a *qualitative* description of experimental observation; a *quantitative* fit could be easily obtained through a suitable adjustment of the values of the model parameters.

We now turn to a study of the effect of polydispersity on the dependence of modulus on draw. At temperatures below the maximum drawing temperatures listed Figure 6, the molecular distribution was found to play no significant role, in accord with experimental observations. The importance of polydispersity at temperatures *higher* than T_{\max} is shown in Figure 7. The continuous lines indicate the results obtained with the present model for monodisperse PE with $M_n = M_w = 9.2 \times 10^6$; the dashed lines are for a polydisperse PE with $M_n = 3.5 \times 10^6$ and $M_w = 9.4 \times 10^6$. The two sets of curves were calculated for two different drawing temperatures, $T = 130$ and $T = 155^\circ\text{C}$, which are above the T_{\max} for the M_w range under study (see Figure 6). The figure clearly indicates that, for a given temperature, the polydisperse sample draws less efficiently than its monodisperse counterpart of the same M_w . This finding, of course, is consistent with, and readily understood in view of, the above finding that each chain length exhibits its own maximum temperature for efficient orientation. The polydisperse network indeed comprises a significant fraction of low molecular weight material

which is here being drawn at temperatures well above its own T_{\max} .

A last remark is in order. In previous publications,^{9,10} we reported that, for each molecular weight, there exists a temperature, T_{opt} , at which the draw ratio of PE reaches a maximum value. Model calculations and experimental data^{9,10} indicate a linear increase of T_{opt} with (the logarithm of) the molecular weight, as is the case for the present T_{\max} (Figure 6). The molecular weight dependency of T_{opt} , however, is more pronounced than that of T_{\max} , and experiments indicate that the two cross at $M_w \approx 4 \times 10^5$. For molecular weights higher than 4×10^5 , $T_{\max} < T_{\text{opt}}$ and an optimization of the maximum drawability at T_{opt} will not necessarily be associated with an improvement in mechanical properties. In the present calculations, crossing of the T_{opt} and T_{\max} lines is found to occur at a much lower M_w value ($\approx 4 \times 10^3$). The latter, if so desired, could be easily fitted to the experimental M_w value through a suitable adjustment of our model parameters (activation energy and volume) for the chain slippage process.

To summarize, we presented a molecular model for the effect of temperature on the efficiency of drawing of flexible polymers. The results obtained clearly indicate the presence of a maximum drawing temperature above which disentangling and recoiling of the polymer chains occurs, leading to reduced efficiency of the orientation process.

That maximum temperature is predicted to increase linearly with (the logarithm of) the weight-average molecular weight. Increased polydispersity is also found to significantly decrease the efficiency of drawing at high temperatures. Although the results presented here relate to polyethylene, the general phenomena addressed are, of course, of broader importance.

References and Notes

- (1) Wang, L.-H.; Porter, R. S.; Kanamoto T. *Polymer* **1990**, *31*, 457.
- (2) Irvine, P. A.; Smith, P. *Macromolecules* **1986**, *19*, 240.
- (3) Postema, A. R.; Smith, P. *Macromolecules* **1990**, *23*, 3296.
- (4) Kuhn, W.; Grun, F. *Kolloid Z.* **1942**, *101*, 248.
- (5) Capaccio, G.; Crompton, T. A.; Ward, I. M. *J. Polym. Sci., Polym. Phys. Ed.* **1980**, *18*, 301.
- (6) Zachariades, A. E.; Mead, W. T.; Porter, R. S. In *Ultra High Modulus Polymers*; Ciferri, A., Ward, I. M., Eds.; Applied Science Publishers: London, 1979; p 77.
- (7) Smith, P.; Lemstra, P. J. *Polymer* **1980**, *21*, 1341.
- (8) (a) Termonia, Y.; Smith, P. *Macromolecules* **1987**, *20*, 835; (b) *Ibid.* **1988**, *21*, 2184.
- (9) Termonia, Y.; Allen, S. R.; Smith, P. *Macromolecules* **1988**, *21*, 3485.
- (10) Smith, P.; Termonia, Y. *Colloid Polym. Sci.* **1992**, *270*, 1085.
- (11) Kanamoto, T.; Ohama, T.; Tanaka, K.; Takeda, M.; Porter, R. S. *Polymer* **1987**, *28*, 1517.
- (12) Smook, J.; Flinterman, M.; Pennings, A. J. *Polym. Bull.* **1980**, *2*, 775.
- (13) Smith, P.; Lemstra, P. J. *J. Mater. Sci.* **1980**, *15*, 505.